Journal Name

ARTICLE TYPE

Cite this: DOI: 00.0000/xxxxxxxxxx

Deuteron NMR investigation on orientational order parameter in polymer dispersed liquid crystal elastomers

Andraž Rešetič*[a], Jerneja Milavec[a], Valentina Domenici[c], Blaž Zupančič[a], Alexej Bubnov[d] and Boštjan Zalar[a,b]

Received Date
Accepted Date

DOI: 00.0000/xxxxxxxxxx

Polymer-dispersed liquid crystal elastomers have been recently introduced as a thermomechanically active composite material, consisting of magnetically oriented liquid crystal elastomer particles incorporated in a cured polymer matrix. Their thermomechanical properties are largely governed by the degree of imprinted particle alignment, which can be assessed by means of deuterium perturbed ^{2}H-NMR. Spectra of samples with various degrees of imprinted particle alignment were recorded and the results simulated using the discrete reorientational exchange model developed for determining the dispersion of liquid crystal elastomer's domain orientational distribution. We show that the model can be applied to measure the orientational distribution of embedded liquid crystal microparticles and successfully determine the orientational order parameter in the composite system. Thermomechanical measurements correlate well with the obtained results, thus additionally confirming the validity of the applied method.

1 Introduction

Liquid crystal elastomers couple orientational properties of liquid crystals with the elastic characteristic of the polymer network, a combination that leads to a material with an ability to reversibly thermomechanically deform as a result of the disordering-ordering transition of its mesogen components[1]. Due to their large shape-changing abilities, liquid crystal elastomers (LCEs) are great candidates for a variety of applications[2–4], especially in actuation industry. The large produced strain and different means of actuation[5,6], in most cases with heat[7–11] or light irradiation[12–15], gives them an advantage over other smart-materials, while numerous novel prototype devices based on LCEs[3] and new scientific achievements[2,16] are only broadening their applicative potential. However, a widespread utilization of LCEs in commercial applications is impeded by their unpractical synthesis methods[17]. The production of LCEs is either restricted to small amounts of arbitrary shaped micro-sized samples[18,19], or to macro-sized specimens of limited geometry, usually of thin-strip shapes[11,20–22]. To overcome these limitations, we recently proposed a new method of producing thermomechanically functionalized rubber material of arbitrary shape and size[23]. The soft-soft composite material, termed polymer dispersed liquid crystal elastomers (PDLCEs), consists of LCE microparticles embedded in a cured polymer matrix. The production process consists of dispersing LCE microparticles in a polymer melt and using a strong external magnetic field for orienting the particles prior to polymerizing the surrounding matrix. We are therefore taking advantage of the anisotropic magnetic susceptibility of LCE's mesogen constituents in order to orient the LCE microparticles with induced magnetic torque, so that their mean nematic director is aligned in the magnetic field's direction. Upon curing, the microparticles retain their orientation and couple to the surrounding matrix, thus transferring their thermomechanical deformation onto the whole composite. The strain output, typically measured at $\lambda \approx 1.12$ for composites with nematic sidechain LCE inclusions, depends largely on the concentration of LCE microparticles, Young's modulus of both the filler material and the surrounding matrix, and on the degree of LCE particle's orientation[23]. Having a good control over the latter is especially important, since the ability of PDLCEs to thermomechanically deform is owed entirely to a well and uniform alignment of LCE microparticles throughout the composite. Therefore an assessment of the orientational order of LCE microparticles is needed to further develop and improve the PDLCE's performance by providing more insight into the alignment process.

In this article we turned to ^{2}H-NMR spectroscopy as the means of measuring and quantifying the LCE microparticle's orientational order parameter of a PDLCE composite. This technique has already been proven as an effective method for carrying out

[a] *J. Stefan Institute, Jamova 39, 1000 Ljubljana, Slovenia. Tel: +386 1 477 3955; E-mail: andraz.resetic@ijs.s;*
[b] *Jozef Stefan International Postgraduate School, Jamova 39, 1000 Ljubljana, Slovenia;*
[c] *Dipartimento di Chimica e Chimica Industriale, Universit'a degli studi di Pisa, via Moruzzi 3, 56126 Pisa, Italy;*
[d] *Institute of Physics of the Czech Academy of Sciences, Na Slovance 1999/2, 18221 Prague, Czech Republic;*

investigations of orientational and dynamic properties of LCE's deuterated constituents[24,25]. We will demonstrate that the evolution of the derived orientational order parameter accurately corresponds to the strength of external orientational magnetic field in which the PDLCEs were prepared. Results will be backed up by corresponding thermomechanical measurements and theoretical calculations.

2 Experimental

Preparation of deuterated polymer dispersed liquid crystal elastomer samples

The LCE pre-polymerization mixture was made by adding 1 mmol of Hydroxymethyl-polysiloxane (Acros Organics), 15 mmol of V1 cross-linker (TCI chemicals), 25 mmol of M4 mesogen (TCI chemicals) and 60 mmol of deuterated M(D)6 mesogen (synthesis reported in[26]), to 2 ml of anhydrous toluene (Figure 1). 30 μl of saturated Pt-catalyst (Acros Organics) was added to the mixture and the content was filtered into a home-made cylindrical form for centrifugation. The Pt-catalyst solution was saturated to prevent possible solution concentration changes due to solute evaporation when stored for future synthesis. The pre-polymerization mixture was filtered into two 1.2 ml flasks and polymerized overnight at 343 K in a homogeneous magnetic field of $B = 11.74$ T, inside a wide bore superconductive magnet (Bruker Advance III 500 MHz). The LCE material needs to be synthesized under an applied magnetic field in order to instil mesogen alignment and the formation of bigger nematically ordered domains, the size of which is assumed to be larger compared to the average size of obtained LCE particles[23]. The ensuing particles are thus considered to be monodomain. The flasks were slightly opened during polymerization, allowing for slow evaporation of toluene. The material was then removed from the flasks, cut into thin (1 mm) pieces and further dried in an oven at 333 K for 24 h.

A reference monodomain LCE material was synthesized using the well known two step Finkelmann procedure[20]. Microparticles obtained from a monodomain material preserve their monodomain nature regardless of their size[23]. Here, the same pre-polymerized mixture was centrifuged at 5500 rpm at 343 K for 70 min, resulting in a partially cross-linked LCE film. The second reaction step consists of cutting the LCE film into shorter strips and mechanically loading them at room temperature. Weights of 3 mg were gradually added until the LCE sample became either completely transparent or no further elongation was seen (usually at loads of 15 mg). The samples were left to dry at room temperature for approximately 2 hours and further cross-linked overnight in an oven at 333 K.

PDLCE composites were prepared by cutting LCE material into smaller pieces (approximately 1×1 mm) and mixing them with PDMS (polydimethylsiloxane – Sylgard® 184 Silicon Elastomer Kit) in a 3 : 1 weight ratio. The mixture was frozen with liquid nitrogen and freeze-fractured into a homogeneous paste. Additional PDMS was then mixed in the paste to reduce the LCE particle weight concentration to $w_{LCE} = 0.50$ and a curing agent was added in a $m_{CA} : m_{PDMS} = 1 : 40$ curing agent to PDMS base ratio. The chosen amounts correspond to PDLCEs that exhibit a maximum strain output[23]. The mixture was evacuated and introduced in a cylindrical mold, producing composites of 2 mm in diameter and 7 mm in length. The samples were polymerized in a superconducting magnet under various magnetic fields in the range of $B = 1.5 - 9$ T. Different magnetic fields were accessed by repositioning the NMR probe away from the $B = 9$ T NMR magnet bore's center using plastic tubular-shaped spacers of various lengths. The probe chamber was beforehand heated to the setting temperature of $T = 330$ K to immediately initiate the setting process. This way the LCE's orientation could be quenched in a semi-oriented state, depending on the strength of the magnetic field. The samples were cured overnight.

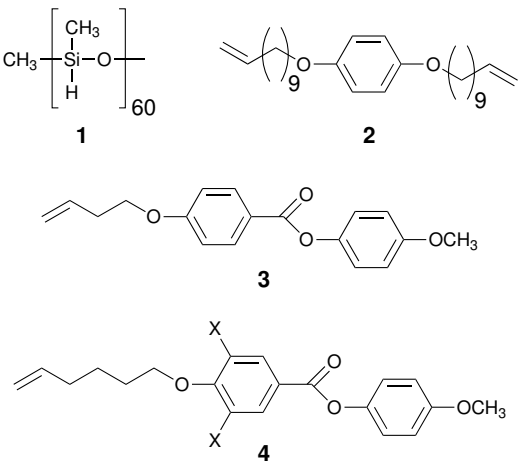

Fig. 1 Compounds used in the synthesis of LCE systems: (1) Hydroxymethyl-polysiloxane polymeric chain, (2) flexible cross-linker V1, (3) nematogen M4 and (4) deuterated nematogen M(D)6, labelled with deuterium at the benzene ring, denoted by X in the molecule schematic.

2.1 ^{2}H-NMR measurements

Measurements were performed with a Bruker Advance III 500 MHz high-resolution solid-state NMR spectrometer, equipped with 11.74 T Bruker Ultrashield superconducting magnet at the Larmor frequency of 76.753 MHz for deuterons. Spectra were recorded by applying a quadrupole echo sequence ($90° - \tau - 90° - \tau_2 - \mathrm{ACQ}$) with a 90° pulse length of 4.8 μs. Echo delay time τ was set from 640 μs to 2.5 μs with decreasing temperature, and delay τ_2 was set to zero. Recycle delay between consecutive acquisitions was set to 25 ms, with 30720 scans performed at each measurement. The measurements were carried on PDLCE samples that were wrapped in a single sheet of Teflon® and inserted into a flat cylindrical coil used for measuring the NMR spectra. The sample was positioned in the center of the coil, perpendicular to the coil axis, so that the instilled particle's nematic director **n** was pointing along the magnetic field. Two rolls of Teflon® tape, approximately the same size as the PDLCE sample, were also packed inside the coil at both sides of the sample to prevent the sample from displacing upon deformation and to completely fill the coil. Spectra of the prepared samples were recorded at 330 K and controlled within 0.1 K accuracy with 5 min for temperature equilibration before every measurement.

3 Results and discussion

3.1 Orientational order parameter of LCE microparticles

Freeze fracturing LCE material produces microparticles that retain the same degree of nematic alignment as the source material, therefore the same nematic director $\mathbf{n}$ can be applied to each individual LCE particle. Considering a polydomain material, the ensuing particles will possess a mean nematic director $<\mathbf{n}>$ that is pointing in the direction of the average alignment of the particle's nematic order. Upon dispersion of LCE microparticles into the polymer melt, the particle's nematic directors are randomly oriented, thus the nematic director distribution is isotropic, $P_0(\cos\vartheta)=\frac{1}{2}$. When LCE particles are aligned in an external applied magnetic field, the orientational anisotropy increases,

$$P_t(\cos\vartheta)=\int_0^1 \delta\left[\cos\vartheta-\cos\vartheta(t,\cos\vartheta_0)\right]d\cos\vartheta_0. \tag{1}$$

Here, t is the time from the start of the director alignment and δ denotes the Dirac Delta function. The term $\cos\vartheta(t,\cos\vartheta_0)$ describes the alignment of a LCE's nematic director, which has its initial orientation at $\vartheta_0\angle(\mathbf{n},\mathbf{B})$ at time t_0. This term is obtained by solving the equation of motion for the given LCE particle. During alignment, the distribution $P_t(\cos\vartheta)$ possesses cylindrical symmetry (independent of azimuthal angle ϕ) about $\mathbf{B}$ and is invariant to the transformation $\vartheta\to\pi-\vartheta$, therefore $\cos\vartheta\in[0,1]$. A global orientational order parameter $Q=\overline{(3\cos^2\vartheta-1)/2}$ is introduced, quantifying the orientational order with the average performed over $P(\cos\vartheta)$. In case of PDLCEs, the order parameter describes the LCE microparticle's orientational ordering and, by taking into account equation (1), it takes the form of:

$$Q(t)=\frac{1}{2}\int_0^1\left[3\cos^2\vartheta(t,\cos\vartheta_0)-1\right]d\cos\vartheta_0. \tag{2}$$

PDLCEs consisting of LCE particles with a well defined nematic order, i.e. monodomain particles, will, when subjected to an external magnetic field $\mathbf{B}$ for a sufficient amount of time, tend to achieve a high orientational order parameter, $Q\to 1$. If the particles are only partially aligned, as may be the case for polydomain particles, at which the particles are aligned by their mean nematic director $<\mathbf{n}>$, or if the surrounding polymer matrix is cured before the orientational process is completed, the PDLCE's order parameter then lies in the range of $0<Q<1$. When no external aligning field is present, the particles remain isotropically oriented and the PDLCE is considered isotropic with $Q=0$.

3.2 Magnetic alignment of LCE microparticles

LCE microparticles can be described as spherical particles, each with its own nematic director. A torque is induced upon the particles by the magnetic field due to the diamagnetic susceptibility of mesogenic molecules. Magnetic torque is described by

$$\Gamma_B=-\frac{1}{\mu_0}V\Delta\chi S_N\mu_0B^2\sin\vartheta\cos\vartheta, \tag{3}$$

where V is the particle's volume, $\Delta\chi$ magnetic susceptibility anisotropy, S_N nematic order parameter and μ_0 the magnetic constant or vacuum permeability. ϑ is the angle between the magnetic field and the nematic director of the LCE particle, $\vartheta\angle(\mathbf{n},\mathbf{B})$. LCE particles also experience an opposite viscous torque from the surrounding matrix,

$$\Gamma_\eta=-\frac{8\pi r^3\eta(t)}{F(r/R)}\frac{d\vartheta}{dt}. \tag{4}$$

$\eta(t)$ denotes the time dependent viscosity of the matrix and $F(r/R)$ the geometrical factor[27], in which r and R are the radii of the short and long axis of the ellipsoid, respectively. For a sphere, where $r/R=1$, factor $F(r/R)$ equals 1, whereas for a moderately deformed sphere, its value is decreased. The LCE particles are assumed spherical, therefore $r\approx R\Rightarrow F\approx 1$, while the particle's moment of inertia is $I=2\rho VR^2/5$, where ρ is the particle's density. The sum of torques can now be written as

$$\alpha_p\tau_\eta^2\frac{d^2\vartheta}{dt^2}=-\sin\vartheta\cos\vartheta-\tau_\eta e^{kt}\frac{d\vartheta}{dt}. \tag{5}$$

We have here defined a new characteristic time $\tau_\eta=6\mu_0\eta_0/(S_N\Delta\chi B^2)$, which describes the particle's alignment time. The exponential term in equation (5) comes from the time depended viscosity, $\eta(t)=\eta_0\exp(kt)$[28], which exponentially increases due to the curing of the polymer melt, the rate of which is determined by the kinetic factor k. A dimensionless particle acceleration term, $\alpha_p=R^2/R_0^2$, with a characteristic radius $R_0=3\eta_0B^{-1}\sqrt{(10\mu_0)/(\rho S_N\Delta\chi)}$ is also introduced. It is seen that for $\alpha_p\ll 1$, which is satisfied for $R_0\gg R$, the left acceleration part in the equation of motion (5) is small enough to be considered zero. For our specific selection of materials ($\eta_0=3.5\,\mathrm{Pas}$ for PDMS, $\rho=10^3\,\mathrm{kgm^{-3}}$, $S_N(T_{room})\approx 0.8$, $\Delta\chi\approx 10^{-7}$ for M4 mesogens and $B\leq 9\,\mathrm{T}$)[29,30] and LCE particle sizes below $100\,\mu\mathrm{m}$, this is indeed the case and the equation of motion can be reduced to

$$\frac{d\vartheta}{dt}\tau_\eta e^{kt}=-\sin\vartheta\cos\vartheta. \tag{6}$$

We will now implement two dimensionless parameters, a dimensionless time $\widetilde{t}=t/\tau_\eta$ and the dimensionless factor $\widetilde{k}=\tau_\eta/\tau_k$, where the latter describes the interplay between the time needed for a successful magnetically driven alignment and the effect of the increasing viscous dampening on the overall particle's alignment time determined by the characteristic time $\tau_k=1/k$. At the moment the particles are subjected to an orientational magnetic field B, their initial angle is defined as $\vartheta(\widetilde{t}=0)=\vartheta_0$ and the particle's angular velocity is $d\vartheta/d\widetilde{t}(\widetilde{t}=0)=0$. Assuming that $\Delta\chi>0\Rightarrow\widetilde{t}(t>0)>0$, the equation of motion (6) has an analytical solution:

$$\cos\vartheta(\widetilde{t},\cos\vartheta_0)=\frac{1}{\sqrt{1+\frac{1-\cos^2\vartheta_0}{\cos^2\vartheta_0}e^{-2/\widetilde{k}\left(1-e^{-\widetilde{k}\widetilde{t}}\right)}}}. \tag{7}$$

With the equation of motion obtained, the new orientational order parameter $Q(\widetilde{t},\widetilde{k})$ is derived via equation (2), resulting in:

$$Q(\widetilde{t},\widetilde{k})=-\frac{1}{2\left(e^{2/\widetilde{k}\left(e^{-\widetilde{k}\widetilde{t}}\right)}-1\right)}\left(2+e^{2/\widetilde{k}\left(e^{-\widetilde{k}\widetilde{t}}\right)}-\frac{3\arctan\sqrt{e^{2/\widetilde{k}\left(e^{-\widetilde{k}\widetilde{t}}\right)}-1}}{\sqrt{e^{2/\widetilde{k}\left(e^{-\widetilde{k}\widetilde{t}}\right)}-1}}\right). \tag{8}$$

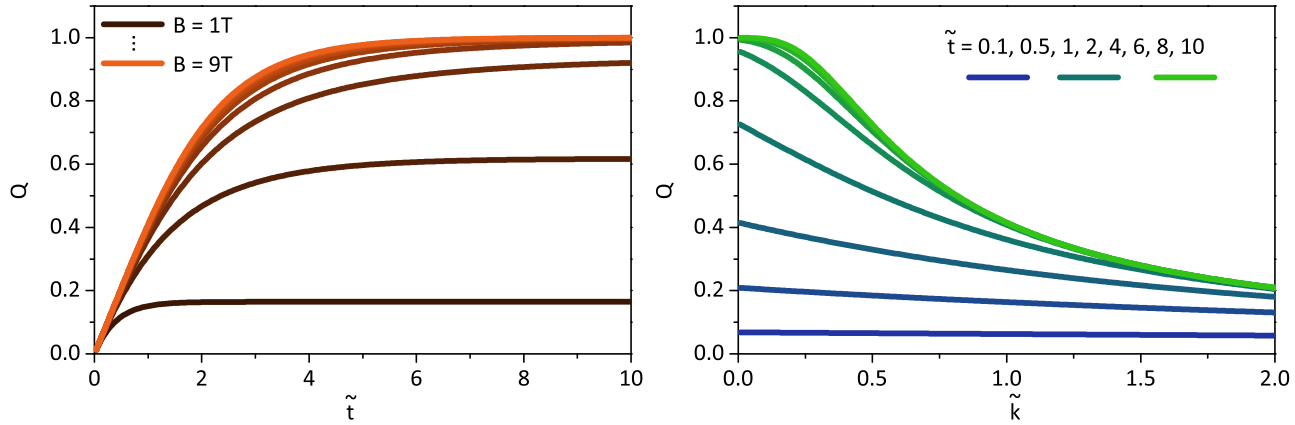

Fig. 2 Evolution of order parameter Q during the alignment process. LCE particles become completely aligned at higher magnetic fields (left graph – orange), while at lower fields ($B < 4\,\mathrm{T}$, dark blue curves), the viscosity locks the particles in place in the semi-aligned state, resulting in a lower saturated value of the order parameter. How well the particles can be aligned is governed by factor $\widetilde{k} = \tau_\eta/\tau_k$ (right graph), which at short times, $\widetilde{t} < 1$ (blue curves), only weakly affects the final Q, while at longer $\widetilde{t} > 1$, the saturated order parameter drops considerably with $\widetilde{k}$, where the LCE particle's alignment is again inhibited by the increased viscosity of the surrounding matrix.

For our choice of materials, the calculation of the order parameter (Figure 2) show that a high orientational order of LCE particles ($Q(\widetilde{t},\widetilde{k}) \to 1$) should be achieved for magnetic fields of $B > 4\,\mathrm{T}$. The maximum value of the PDLCE's order parameter always saturates at $\widetilde{t} \geq 9$, regardless of the magnetic field strength, but the order parameter reached is lowered on the account of the particles being locked in place by the increasing viscosity of the curing matrix before their complete alignment (alignment time τ is faster than the polymerization rate τ_k). The value for the kinetic factor, $k = 0.253\,\mathrm{min}^{-1}$, of the curing matrix was estimated from investigations in[31], performed on the same silicone material as used in our experiments. If the kinetic factor was lower, a high orientational order would be achieved even for lower magnetic field strengths or, in the case of UV-curable polymer where the polymerization can be triggered at any point during the alignment process, we could, if given enough time, achieve efficient ordering at almost arbitrary applied magnetic fields, as long as the induced magnetic torque of the particle is greater than the viscous torque.

3.3 Determining the Orientational Order Parameter Q

Since LCE particles retain the nematic alignment of the initial LCE material from which they are made of, the recorded quadrupole-perturbed deuterated NMR spectra also pertains a similar spectral shape as it's deuteraded components, i.e. a quadrupole spectral splitting, related to the local mesogen nematic order parameter S[32–34]:

$$\nu^{\pm} = \pm\frac{3}{4}\nu_q S P_2(\cos\beta)\,P_2(\cos\theta) = \pm\frac{3}{4}\bar{\nu}_q S P_2(\cos\theta)\,. \qquad (9)$$

Here, ν_q is the quadrupole frequency of the deuteron in a C-^{2}H bond and P_2 are the second Legendre polynomial. Angle β is the angle between the molecular long axis and the C-^{2}H bond and θ the angle between the long molecular axis and the magnetic field. For deuterated M(D)6 mesogen, the deuteration sites are located at the phenyl ring, where $\beta = 60°$ and the respective effective quadrupole frequency is $\bar{\nu}_q \approx 22\,\mathrm{kHz}$. A nematic director $\mathbf{n}$ can be attributed to each individual LCE particle, pointing in the direction of their mesogenic nematic ordering. If a magnetic field is present, the LCE particles reorient so that their nematic director aligns with the field direction. Evaluations on the degree of instilled order are realized by recording the ^{2}H-NMR spectra of cured PDLCEs and simulating the spectra with the discrete reorientational exchange model, described in greater detail in[29], in which it was utilized for determination of the degree of nematic domain alignment in deuterated LCEs. We will show that the same model can also be applied to PDLCE's to estimate the orientational ordering of LCE microparticles. In the model, the domain's nematic director alignment is quantified by the dispersion of orientational distribution, σ_θ, originating from the presumed spherical Gaussian distribution of the domain's nematic director's orientations:

$$w(u,\sigma_u) = \frac{e^{-\frac{1-u^2}{2\sigma_u^2}}}{e^{-\frac{1}{2\sigma_u^2}}\sqrt{2\pi\sigma_u}\,\mathrm{erfi}\left(\frac{1}{\sqrt{2}\sigma_u}\right)} \qquad (10)$$

Variable u denotes the orientation angle of a given domain with respect to the magnetic field direction, $u = \cos\theta \in [-1,1]$, and $\sigma_u \in [0,\infty]$ is the degree of dispersion of domain orientation distribution. The dispersion term σ_u is defined as $\tan\sigma_\theta = \sigma_u$, where it is expressed in degrees of angle θ inside the interval of $\sigma_\theta \in [0°, 90°]$. Value $\sigma_\theta = 0°$ is associated with a perfectly aligned nematic director over the whole LCE specimen, whereas $\sigma_\theta = 90°$ describes isotropically oriented mesogens. If we presume that LCE particles are monodomain, the two σ_θ values are, regarding PDLCEs, respectively equivalent to scenarios where all the particles are either completely aligned (their nematic directors are oriented in the same direction), or completely unoriented, where no preferable orientation of nematic directors is present. The model also estimates the influence of the reorientational exchange, i.e, impact of molecular dynamic processes on the motional averaging of the ensuing ^{2}H-NMR spectra, described in the model by

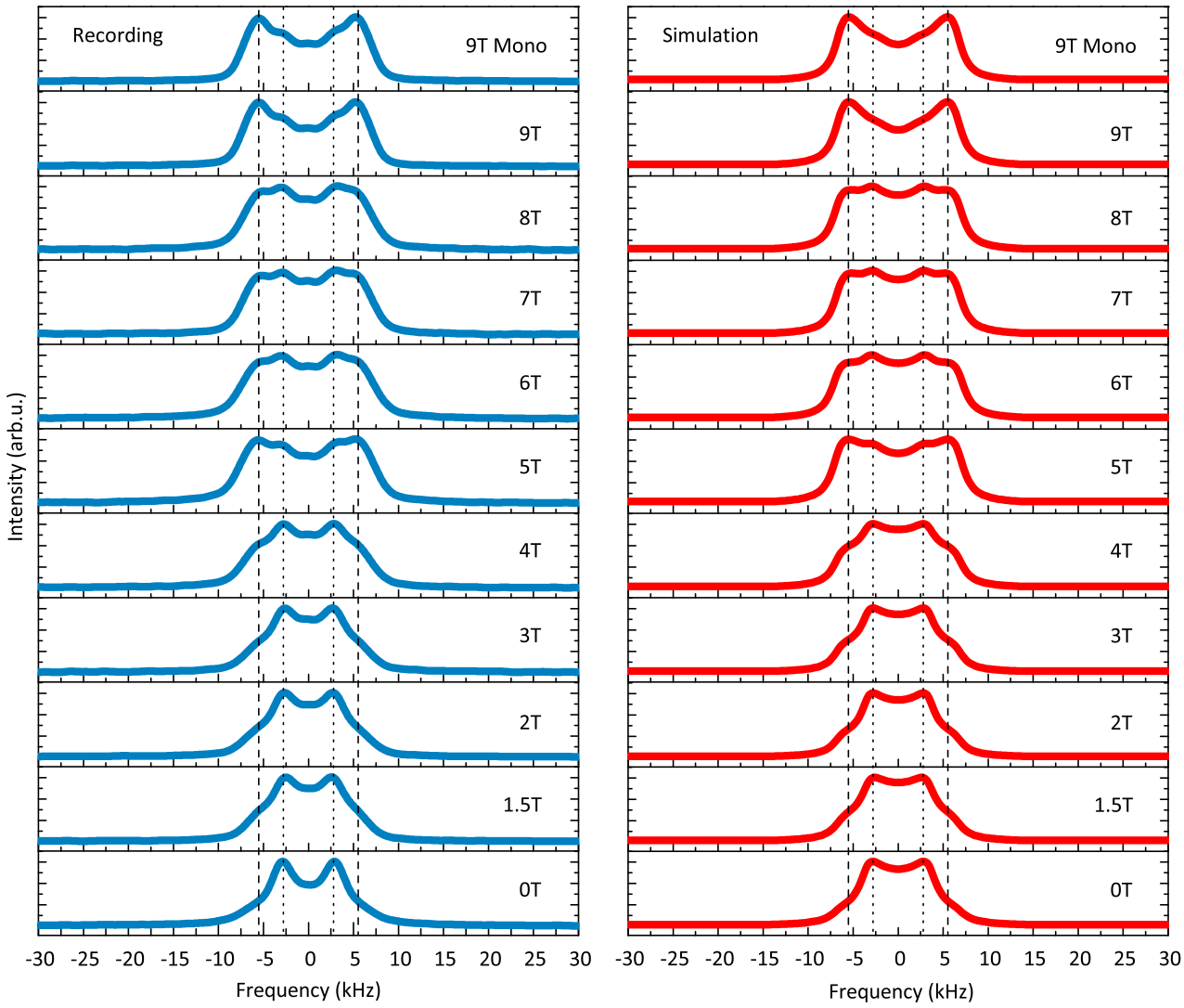

Fig. 3 Recorded and simulated spectra of deuterated PDLCEs. Recorded spectra (blue) exhibit two splittings: at $\nu = \pm 3\,\mathrm{kHz}$, associated with unoriented LCE particles, and at $\nu = \pm 6\,\mathrm{kHz}$, at which peaks become more pronounced with better particle alignment against the magnetic field. Measured spectra were simulated (red) to derive the orientational distribution σ_θ, needed for assessment of the order parameter Q. Simulations match the recorded spectra to a maximum of 20% error margin.

the motional effectiveness parameter α. When in the "fast motion" regime ($\alpha \gg 1$), the LCE's molecular components exhibit fast reorientational dynamics, resulting in an averaged out homogeneous Lorenzian spectral line due to motional narrowing. This is seen at higher temperatures, when the LCE is in the isotropic phase. In the "slow motion" regime ($\alpha \ll 1$), there is no motional averaging and the spectrum is inhomogeneously broadened. The determination of the orientational order parameter has been carried in this low temperature regime, where the particles exhibit a high nematic order parameter S and the effects of the molecular dynamics on the obtained spectra are disregarded. When the PDLCE sample is positioned in the same geometry against the magnetic field during NMR investigations as it was during the aligning process, so that $u = \cos 0^\circ = 1$, then the shape of the spectra is governed only by the dispersion of orientational distribution σ_θ. Values of parameter σ_θ can now be estimated by modelling the experimental spectral patterns and used to asses the LCE particle's orientational order parameter, $Q(\sigma_\theta)$, which takes the form of:

$$\begin{aligned} Q(\sigma_\theta) &= \int_{-1}^{1} w(u, \tan\sigma_\theta)\frac{(3u^2-1)}{2}du \\ &= -\frac{1}{2} - \tan(\sigma_\theta)\left(\frac{3\tan(\sigma_\theta)}{2} - \frac{3\exp\left(\frac{\cot^2(\sigma_\theta)}{2}\right)}{\sqrt{2\pi}\,\mathrm{erfi}\left(\frac{\cot(\sigma_\theta)}{\sqrt{2}}\right)}\right). \end{aligned} \tag{11}$$

Spectra of PDLCEs prepared under different magnetic fields were all recorded at the composite's setting temperature ($T_0 = 330\,\mathrm{K}$) to eliminate possible internal stresses arising from non-matching strains between the polymer matrix and LCE particles. These locally induced mechanical fields can skew the particle's alignment, leading to a false determination of the imprinted order parameter Q. The recorded spectra are presented in Figure 3 (blue), along with their simulated counterparts (red) computed

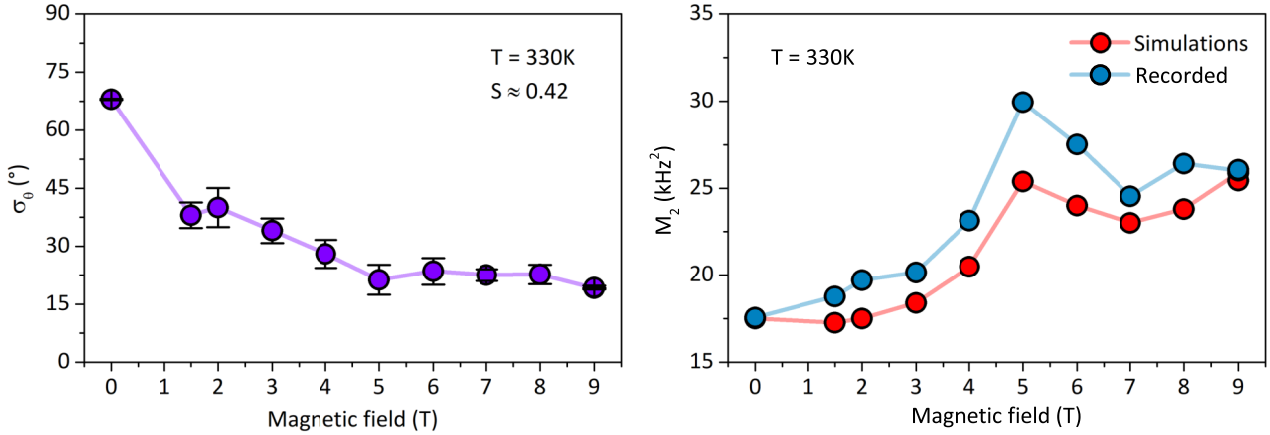

Fig. 4 Derived orientational distribution σ_θ with associated second moment M_2. LCEs alignment increases with magnetic field and consequently the orientational distribution σ_θ decreases until it reaches a constant value at $B = 5\,\mathrm{T}$, at which point the order parameter reaches its maximum value. Error bars were determined from the difference between the calculated second moments M_2 of recorded and simulated spectra (right graph).

using the discrete reorientational exchange model[29]. Measurements show a spectral splitting that is characteristic of an LC system. For the unoriented PDLCE (denoted by $B = 0\,\mathrm{T}$) the splitting is minimum with peaks positioned at $\nu = \pm 3\,\mathrm{kHz}$, signifying a random distribution of particle's nematic director orientations. Outer peaks positioned at $\nu = \pm 6\,\mathrm{kHz}$ start to form and gain on intensity with higher magnetic field strengths, indicating that the particle's orientational order is increasing. The majority of the particles becomes aligned when the outer peak's intensity surpasses the inner, which in our case can only be observed for $B = 9\,\mathrm{T}$. A saturation of orientational order is seen at $B \geq 5\,\mathrm{T}$, where the intensity of both the inner and outer peaks are approximately the same, meaning that some disordering still remains in the composite. An additional measurement was also made of the composite containing two-step synthesized LCEs (termed MONO in Figure 3) in order to override the suspicion of magnetically synthesized particles being prevalently multi-domain, and thus non-reorientable, since both spectra at $B = 9\,\mathrm{T}$ match very well.

The dispersion of orientational distribution σ_θ (Figure 4 – left graph) is derived from the simulated spectra. The orientational dispersion changes almost linearly from $\sigma_\theta = 65°$ at zero field, to a saturated value of $\sigma_\theta = 20°$ for fields above $B = 5\,\mathrm{T}$, where the maximum ordering is also achieved. The error bars are determined from the modelling precision of the simulated spectra and were calculated as the difference between the truncated second moments $M_2 = \int_{-\nu_{tr}}^{+\nu_{tr}} \nu^2 \mathscr{J}(\nu) d\nu$ of the recorded and simulated spectral lines (where $\mathscr{J}(\nu)$ is the spectral intensity). These differ by a maximum of $\sim$ 20% error margin (see Figure 4 – right graph). The results for PDLCEs with magnetically and two-step synthesized LCE microparticles at $B = 9\,\mathrm{T}$ almost completely overlap, showing more clearly that there is no reason to suspect that different synthesis procedure affect the results.

Using Equation (11), the orientational order parameter $Q(\sigma_\theta)$ can now be determined from the derived orientational distributions σ_θ (blue circles in Figure 5, left graph). The results are fitted (blue line in Figure 5, left graph) with a simulated curve, $y = AQ(\widetilde{t}, \widetilde{k})$ (see Equation (8)), which includes an additional constant the orientability parameter $0 \leq A \leq 1$. A accounts for diminished order in a real system where either LCE microparticle orientability is restricted at high particle concentrations or the particles are not ideally monodomain, so that ideal alignment cannot be reached even in the $Q(\widetilde{t} = \infty, \widetilde{k} = 0) = 1$ limit. Parameters $\widetilde{k}$ and τ_η were calculated from determined magnetic fields and known material properties, while the duration of the alignment process t, found in $\widetilde{t} = t/\tau_\eta$, and parameter A were altered to effectively match the results. The best fit was obtained for parameter values of $A = 0.49$ and $t = 1.2\,\mathrm{min}$.

One can see that the order parameter $Q(\sigma_\theta)$ increases with magnetic field to a constant value of $Q_{max}(\sigma_\theta) = 0.54$ for $B \geq 5\,\mathrm{T}$, signifying a maximum reached LCE particle alignment. Right graph in Figure 5 shows the thermomechanical measurements performed on the same samples. When compared to the evolution of the order parameter, the PDLCEs thermomechanical response directly correlates with the degree of imprinted particle alignment, i.e. the magnitude of sample deformation is increased with the magnetic field and a maximum deformation ($\lambda_{max}(T) \to 1.08$) is seen for $B \geq 5\,\mathrm{T}$. This confirms the validity of our model to accurately evaluate the orientational order parameter. By allowing to have an overview over the LCE microparticle ordering, the alignment process parameters can now be precisely controlled in order to produce PDLCEs with custom-tailored thermomechanical properties.

Still, the relatively low values of $Q_{max}(\sigma_\theta)$ and parameters A and t from the simulated curve suggest that only partial particle alignment is achieved. Assuring a high particle ordering would further improve the PDLCE's thremomechanical performance. An efficient ordering can be hindered by the high concentration of LCE microparticles used in PDLCE mixture preparation ($w_{LCE} = 0.50$). Due to their high packing, the LCE particles simply lack the space needed to successfully align. To investigate this claim, we performed additional measurements of a PDLCE specimen with lower microparticle concentration of $w_{LCE} = 0.20$, oriented in a $B = 9\,\mathrm{T}$ magnetic field. The resulting NMR spectra in Figure 6 exhibits no internal peaks, suggesting a well aligned particle formation is achieved, in contrast to an equivalent PDLCE sample containing monodomain particles (9T MONO), where a

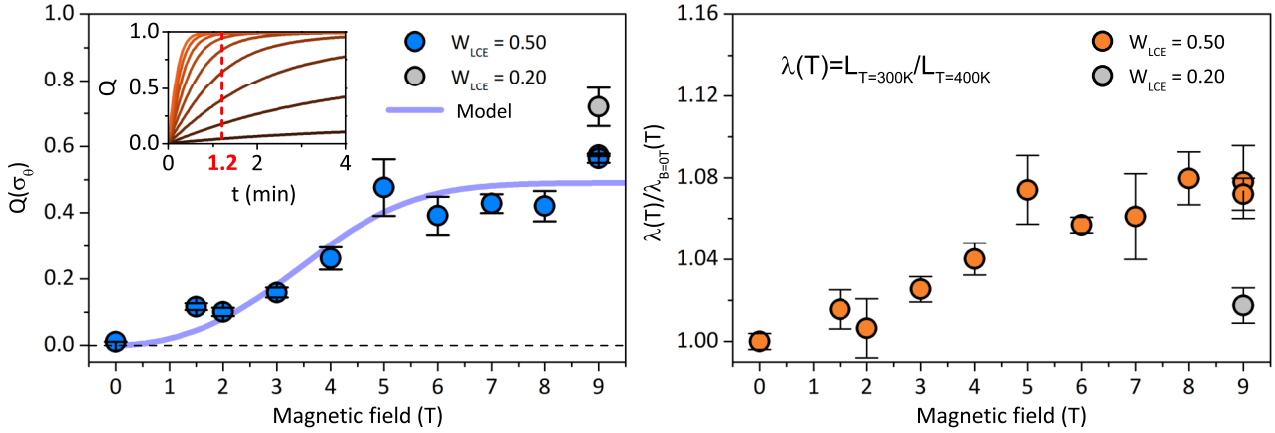

Fig. 5 Experimentally determined orientational order parameter $Q(\sigma_\theta)$ (left graph) and thermomechanical response (right graph) of the same PDLCE samples. The maximum order parameter is reached for $B \geq 5\,\mathrm{T}$ at the value of $Q_{max}(\sigma_\theta) = 0.54$. Graph inset (left graph) shows the time evolution of the order parameter Q , calculated for corresponding magnetic fields of $9\,\mathrm{T}$ to $1\,\mathrm{T}$ (orange to blue line, respectively). Best fit for the simulated curve (blue line) was found as if the whole alignment process was halted at $t = 1.2\,\mathrm{min}$ (graph inset - red dashed line). Thermomechanical responses (right graph) were determined on several pieces of the same sample by measuring the length change when heated from $300\,\mathrm{K}$ to $400\,\mathrm{K}$. Grey circles correspond to measurements of PDLCE with $w_{LCE} = 0.20$.

fraction of particles remain unoriented. When analysed, the derived order parameter for the lower concentrated system (grey circles in Figure 5) is much higher - $Q_{w_{el}=0.20}(\sigma_\theta) = 0.72$, compared to the maximum observed $Q_{max}(\sigma_\theta) = 0.54$. Nevertheless, a sufficient amount of LCE material is still needed for any significant thermomechanical response, as indicated in Figure 5 (right graph), where only $\lambda(T) \rightarrow 1.02$ is observed for the $w_{LCE} = 0.20$ sample. We therefore believe that the degree of particle alignment is mostly hindered by the multi-domain nature of the LCE microparticles. For instance, poyldomain particles cannot be fully aligned due to the high dispersion of their individual domain nematic directors. PDLCEs made from such particles would exhibit a lower $Q(\sigma_\theta)$ and a proportionally reduced thermomechanical response. Since the order parameter $Q(\sigma_\theta)\,|_{B=9\,\mathrm{T}}$ for PDLCEs consisting of magnetically and two-step synthesized LCE particles is nearly the same, we suspect that the synthesis process is not the source of LCE particle's polydomain nature, but rather particle aggregation or domain fragmentation from large mechanical forces present during the milling process. Other factors, such as non-uniform shape and size distribution, or particle's reduced internal nematic ordering at the setting temperature ($330\,\mathrm{K}$) can also be detrimental to their orientability. Even without taking the above mentioned parameters into consideration, our model still successfully describes the behaviour and impact of the matrix's viscosity and applied magnetic fields on the PDLCE's orientational order parameter.

4 Conclusions

By employing ^{2}H-NMR spectroscopy, we successfully determined the orientational order parameter Q that describes the degree of instilled LCE microparticle alignment inside a PDLCE composite. The splitting and the shape of the recorded spectral lines are proportional to the LCE's mean nematic director orientation against the magnetic field and can thus be used to address the magnitude of LCE particle ordering. PDLCE composites with differ-

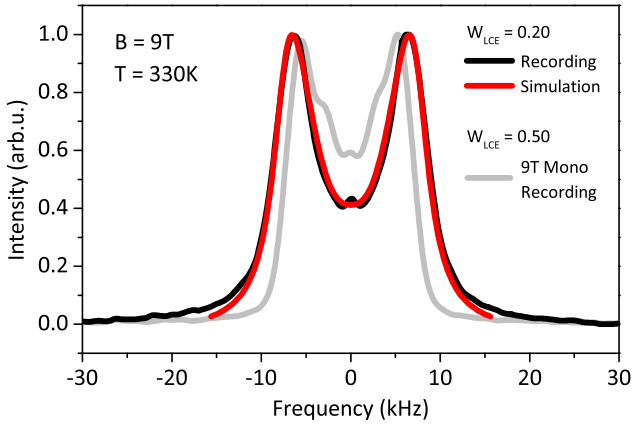

Fig. 6 Comparison of recorded ^{2}H-NMR spectra between PDLCE samples with $w_{LCE} = 0.20$ and $w_{LCE} = 0.50$ LCE microparticle content. Lower concentrated sample (black lines) shows two well separated spectral lines, while additional internal peaks associated with greater microparticle's orientational disordering are observed for higher concentrated sample (grey lines). Discrepancies between the outer spectral line splitting originate from a slight difference in the LCE material's nematic order parameter S_N. Spectra of $w_{LCE} = 0.20$ sample was simulated (red line) using $S_N = 0.47$ and $\sigma_\theta = 16°$.

ently instilled orientational order parameter were produced by aligning and curing the PDLCE mixture in various magnetic field strengths (from $B = 1\,\mathrm{T}$ to $B = 9\,\mathrm{T}$). Deuterium quadrupole perturbed ^{2}H-NMR spectra were then recorded and simulated using the discrete reorientational exchange model[29] to obtain the dispersion of orientational distribution σ_θ, a quantitative measurement of LCE particle domain's nematic director alignment against the NMR's magnetic field direction. Measured values were used to estimate the orientational order parameter $Q(\sigma_\theta)$ and the results compared with theoretical calculations, at which the predicted order parameter $Q(\widetilde{t},\widetilde{k})$ is determined by the alignment time of individual LCE particles (expressed as $\widetilde{t}$) and the polymerization

rate of the curing PDMS matrix (described by factor $\widetilde{k}$). Measurements show a decrease in the orientational dispersion σ_θ with increasing magnetic field strength, settling at a constant value of $\sigma_\theta = 20^\circ$ at $B \geq 5$T, at which point a maximum particle ordering is reached. The derived order parameter $Q(\sigma_\theta)$ rises accordingly with the magnetic field and converges around the maximum value of $Q_{max}(\sigma_\theta) = 0.54$. The composite's thermomechanical response follows the same dependency, establishing a good correlation between thermomechanical output and the degree of particle alignment. Discrepancies observed between the maximum limits of predicted and evaluated order parameter values are shown to mostly originate from the high packing of LCE microparticles and their polydomain nature. Since high concentration of LCE filler material is imperative for a sufficient thermomechanical response, using monodomain LCE particles of homogeneous size and geometry in PDLCE production would result in a much higher orientational ordering and a significant improvement to the composite's thermomechanical deformation rate.

Conflicts of interest

There are no conflicts to declare.

Acknowledgements

This research was partially supported by the Czech Science Foundation [Project No. CSF 19-03564S] and the Ministry of Education, Youth and Sports of the Czech Republic [Project No. LTC19051]. The author (A.B.) would like to acknowledge the contribution of the COST Action CA17139 and Operational Programme Research, Development and Education financed by European Structural and Investment Funds and the Czech Ministry of Education, Youth and Sports [Project No. SOLID21 - CZ.02.1.01/0.0/0.0/16_019/0000760].

Notes and references

1 M. Warner and E. M. Terentjev, *Liquid Crystal Elastomers*, Oxford University Press, USA, 2003.
2 S. W. Ula, N. A. Traugutt, R. H. Volpe, R. R. Patel, K. Yu and C. M. Yakacki, *Liquid Crystals Reviews*, 2018, **6**, 78–107.
3 W. H. d. Jeu, *Liquid Crystal Elastomers: Materials and Applications*, Springer, 2012.
4 C. Ohm, M. Brehmer and R. Zentel, *Advanced Materials*, 2010, **22**, 3366–3387.
5 P. Xie and R. Zhang, *Journal of Materials Chemistry*, 2005, **15**, 2529–2550.
6 T. J. White and D. J. Broer, *Nature Materials*, 2015, **14**, 1087–1098.
7 D. L. Thomsen, P. Keller, J. Naciri, R. Pink, H. Jeon, D. Shenoy and B. R. Ratna, *Macromolecules*, 2001, **34**, 5868–5875.
8 A. R. Tajbakhsh and E. M. Terentjev, *The European Physical Journal E*, 2001, **6**, 181–188.
9 M. Chambers, H. Finkelmann, M. Remškar, A. Sánchez-Ferrer, B. Zalar and S. Žumer, *Journal of Materials Chemistry*, 2009, **19**, 1524–1531.
10 Y. Sawa, K. Urayama, T. Takigawa, A. DeSimone and L. Teresi, *Macromolecules*, 2010, **43**, 4362–4369.
11 A. Rešetič, J. Milavec, V. Domenici, B. Zupančič, A. Bubnov and B. Zalar, *Polymer*, 2018, **158**, 96–102.
12 M.-H. Li, P. Keller, B. Li, X. Wang and M. Brunet, *Advanced Materials*, 2003, **15**, 569–572.
13 P. M. Hogan, A. R. Tajbakhsh and E. M. Terentjev, *Physical Review E*, 2002, **65**, 041720.
14 M. Camacho-Lopez, H. Finkelmann, P. Palffy-Muhoray and M. Shelley, *Nature Materials*, 2004, **3**, 307–310.
15 H. Zeng, M. Lahikainen, O. M. Wani, A. Berdin and A. Priimagi, *Photoactive Functional Soft Materials*, John Wiley & Sons, Ltd, 2018, pp. 197–226.
16 Z. Pei, Y. Yang, Q. Chen, E. M. Terentjev, Y. Wei and Y. Ji, *Nature Materials*, 2014, **13**, 36–41.
17 R. S. Kularatne, H. Kim, J. M. Boothby and T. H. Ware, *Journal of Polymer Science Part B: Polymer Physics*, 2017, **55**, 395–411.
18 H. Zeng, P. Wasylczyk, G. Cerretti, D. Martella, C. Parmeggiani and D. S. Wiersma, *Applied Physics Letters*, 2015, **106**, 111902.
19 L. B. Braun and R. Zentel, *Liquid Crystals*, 2019, **46**, 2023–2041.
20 J. Küpfer and H. Finkelmann, *Die Makromolekulare Chemie, Rapid Communications*, 1991, **12**, 717–726.
21 M. O. Saed, A. H. Torbati, D. P. Nair and C. M. Yakacki, *JoVE (Journal of Visualized Experiments)*, 2016, e53546–e53546.
22 T. H. Ware, M. E. McConney, J. J. Wie, V. P. Tondiglia and T. J. White, *Science*, 2015, **347**, 982–984.
23 A. Rešetič, J. Milavec, B. Zupančič, V. Domenici and B. Zalar, *Nature Communications*, 2016, **7**, 13140.
24 V. Domenici, J. Milavec, B. Zupančič, A. Bubnov, V. Hamplova and B. Zalar, *Magnetic Resonance in Chemistry*, 2014, **52**, 649–655.
25 J. Milavec, A. Resetic, A. Bubnov, B. Zalar and V. Domenici, *Liquid Crystals*, 2018, **45**, 2158–2173.
26 V. Domenici, J. Milavec, A. Bubnov, D. Pociecha, B. Zupančič, A. Rešetič, V. Hamplová, E. Gorecka and B. Zalar, *RSC Advances*, 2014, **4**, 44056–44064.
27 R. A. Pethrick, *British Polymer Journal*, 1988, **20**, 299–299.
28 M. B. Roller, *Polymer Engineering & Science*, 1975, **15**, 406–414.
29 J. Milavec, V. Domenici, B. Zupančič, A. Rešetič, A. Bubnov and B. Zalar, *Phys. Chem. Chem. Phys.*, 2016, **18**, 4071–4077.
30 H. Schad, G. Baur and G. Meier, *The Journal of Chemical Physics*, 1979, **71**, 3174–3181.
31 F. Schneider, J. Draheim, R. Kamberger and U. Wallrabe, *Sensors and Actuators A: Physical*, 2009, **151**, 95–99.
32 R. Y. Dong, *Nuclear Magnetic Resonance of Liquid Crystals*, Springer, 2nd edn, 1997.
33 J. Emsley, *Nuclear Magnetic Resonance of Liquid Crystals*, Springer Science & Business Media, 2012.
34 V. Domenici, *Progress in Nuclear Magnetic Resonance Spectroscopy*, 2012, **63**, 1–32.